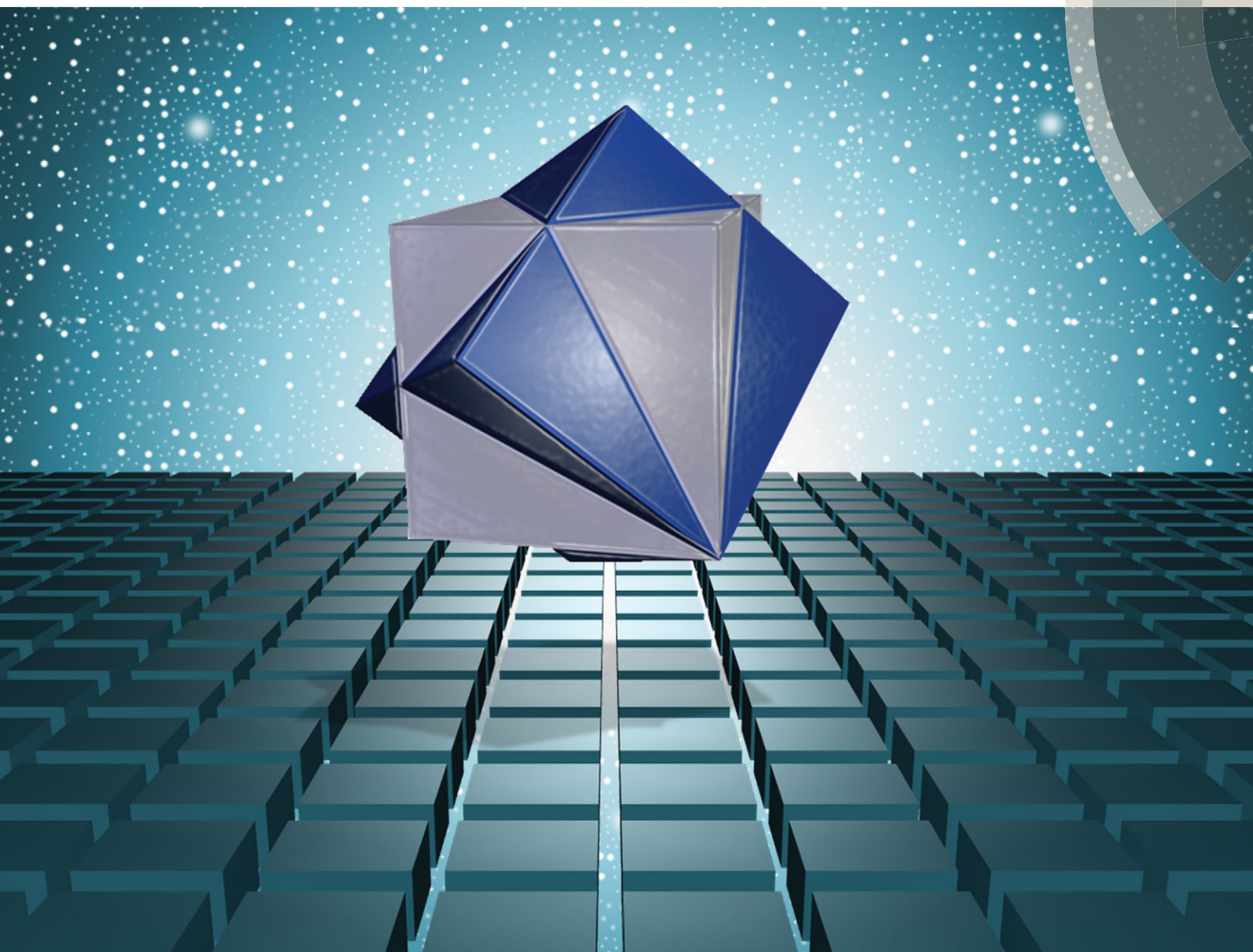


# ChemComm

Chemical Communications

[www.rsc.org/chemcomm](http://www.rsc.org/chemcomm)



ISSN 1359-7345



ROYAL SOCIETY  
OF CHEMISTRY

## COMMUNICATION

Michael J. Zaworotko *et al.*

Novel mode of 2-fold interpenetration observed in a primitive cubic network of formula  $[\text{Ni}(\text{1,2-bis(4-pyridyl)acetylene})_2(\text{Cr}_2\text{O}_7)]_n$



Cite this: *Chem. Commun.*, 2015, 51, 14832

Received 15th July 2015,  
Accepted 19th August 2015

DOI: 10.1039/c5cc05866j

www.rsc.org/chemcomm

# Novel mode of 2-fold interpenetration observed in a primitive cubic network of formula $[\text{Ni}(\text{1,2-bis(4-pyridyl)acetylene})_2(\text{Cr}_2\text{O}_7)]_n$ †

Hayley S. Scott,<sup>a</sup> Alankriti Bajpai,<sup>a</sup> Kai-Jie Chen,<sup>a</sup> Tony Pham,<sup>b</sup> Brian Space,<sup>b</sup> John J. Perry IV<sup>a</sup> and Michael J. Zaworotko<sup>\*a</sup>

A primitive cubic (pcu) network of formula  $[\text{Ni}(\text{1,2-bis(4-pyridyl)acetylene})_2(\text{Cr}_2\text{O}_7)]_n$ , **DICRO-2-Ni-i**, has been synthesised and found to exhibit a novel type of inclined 2-fold interpenetration and an isosteric heat of adsorption ( $Q_{\text{st}}$ ) of  $30.5 \text{ kJ mol}^{-1}$  towards  $\text{CO}_2$  at zero loading.  $Q_{\text{st}}$  is relatively high in the broad context but less than that observed in related hybrid ultramicroporous materials, a feature that can be understood after studying pore structure and molecular simulations of  $\text{CO}_2$  adsorption.

Our understanding of how molecular structure influences crystal packing, crystal structure and, therefore, physicochemical properties has progressed steadily over the past two decades. Now, crystal engineering<sup>1</sup> offers a number of rational design strategies for the creation of new families of crystalline materials with desired functional properties. Metal-organic materials (MOMs),<sup>2</sup> also known as coordination polymers or metal-organic frameworks,<sup>3</sup> represent a broad class of materials particularly suited to the principles of crystal engineering as their modular nature lends itself to systematic study of properties of relevance to applications as diverse as gas separation and storage,<sup>4</sup> catalysis,<sup>5</sup> small-molecule separation<sup>6</sup> and chemical sensing.<sup>7</sup> An important subclass of MOMs is emerging, which combines two features that can enhance sorbent-sorbate interactions: the presence of inorganic anions that offer strong electrostatics when compared with organic linker ligands; ultramicropores ( $<0.7 \text{ nm}$ ) that offer a good fit for important sorbates such as  $\text{CO}_2$  and  $\text{CH}_4$ . This subclass, which could be termed Hybrid Ultramicroporous Materials, or HUMs, have recently been found to exhibit benchmark selectivity for small polar gases such as  $\text{CO}_2$  over competing less polar gases like  $\text{N}_2$ .<sup>8</sup>

Two families of HUMs or “HUM platforms” have been developed by our group. The first platform is derived from parent materials comprised from square lattice (**sql**) nets constructed from transition metals and dipyrindyl ligands<sup>9</sup> pillared with hexafluorometallate anions (*i.e.*  $\text{SiF}_6^{2-}$ ,  $\text{TiF}_6^{2-}$ , *etc.*)<sup>10</sup> to generate **pcu** structures with pores ranging from  $<0.4 \text{ nm}$  to  $>1.3 \text{ nm}$ .<sup>8</sup> The second platform is also based upon **sql** nets built from transition metals and dipyrindyl ligands, but the inorganic pillar is chromate, molybdate or tungstate ( $\text{CrO}_4^{2-}$ ,  $\text{MoO}_4^{2-}$  or  $\text{WO}_4^{2-}$ ). These oxyanions serve as angular pillars and afford structures that adopt a novel topology, **mmo**.<sup>8a,b</sup> Aiming to expand the scope of HUMs, we analysed the Cambridge structural database (CSD),<sup>11</sup> which revealed a potential platform based upon dichromate pillars: **pcu** networks derived from  $[\text{M}^{\text{II}}(\text{4,4'-bipyridine})_2(\text{Cr}_2\text{O}_7)]_n$ , (where  $\text{M} = \text{Fe}^{2+}$ ,  $\text{Co}^{2+}$ ,  $\text{Ni}^{2+}$ ,  $\text{Cu}^{2+}$ ).<sup>12</sup> To adopt a consistent nomenclature, we have named this platform of materials **DICRO-X-M**, where **DICRO** = dichromate anion, **X** = ligand, numbered by order of publication and **M** = transition metal. In the case of interpenetration **-i** is appended. Using this nomenclature, the previously published structures belong to the subset **DICRO-1-M-i**.

We report herein the second subset of this platform,  $[\text{Ni}(\text{1,2-bis(4-pyridyl)acetylene})_2(\text{Cr}_2\text{O}_7)]_n$  **DICRO-2-Ni-i** (Fig. 1), a 2-fold

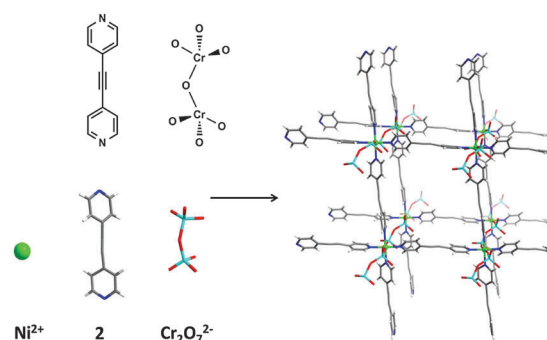


Fig. 1 **DICRO-2-Ni-i** is formed by self-assembly of octahedral  $\text{Ni}^{2+}$  centres (green), organic linkers (**2**) (grey C and dark blue N) and dichromate anions that serve the role of pillars (light blue Cr and red O).

<sup>a</sup> Department of Chemical and Environmental Science, Materials and Surface Science Institute, University of Limerick, Republic of Ireland. E-mail: xtal@ul.ie

<sup>b</sup> Department of Chemistry, CHE 205, University of South Florida, 4202 East Fowler Avenue, Tampa, Florida 33620, USA

† Electronic supplementary information (ESI) available: Complete synthetic protocol, compound characterisation and crystallographic details. CCDC 1412848. For ESI and crystallographic data in CIF or other electronic format see DOI: 10.1039/c5cc05866j

interpenetrated structure that represents the first example of a **pcu** network in which the frameworks are orientated in an inclined arrangement, resulting in a 1D channel running through the structure. **DICRO-2-Ni-i** was characterised by single-crystal and powder X-ray diffraction, thermogravimetric analysis, FT-IR spectroscopy and gas sorption measurements ( $\text{CO}_2$  and  $\text{N}_2$ ). In addition, molecular simulations of  $\text{CO}_2$  adsorption were conducted in order to enable interpretation of the experimental gas sorption measurements.

**DICRO-2-Ni-i** was synthesised at room temperature (see ESI†) by layering an aqueous solution of  $\text{NiCl}_2/\text{K}_2\text{Cr}_2\text{O}_7$  over an acetonitrile solution of ligand **2** (see Fig. 1). The crystal structure of the resulting product was determined by single-crystal X-ray diffraction (ESI†) from data collected at 100 K and found to crystallise in the orthorhombic space group *I*222. Powder X-ray diffraction experiments (ESI†) indicate that the bulk material obtained from slow-diffusion layering consisted of a single phase and that this phase matches the pattern calculated from the structure determined from single-crystal X-ray diffraction. Thermal stability measurements (ESI†) reveal that **DICRO-2-Ni-i** is stable up to *ca.* 200 °C, after which point it undergoes significant weight loss attributable to decomposition (Fig. S2, ESI†).

In **DICRO-2-Ni-i**, each  $\text{Ni}^{2+}$  cation adopts octahedral coordination geometry: four nitrogen atoms from four different dipyriddy linker ligands (**2** in Fig. 1) form the equatorial plane with an average Ni–N bond distance of 2.049(16) Å; ligand **2** exhibits a torsion angle of 53.3° between pyridyl groups. The octahedral coordination geometry is completed with two oxygen atoms from two different dichromate anions ( $\text{Cr}_2\text{O}_7^{2-}$ ) that bind at the axial positions of the  $\text{Ni}^{2+}$  cations with Ni–O bond distances of 2.018(13) Å. These distances correspond closely with the value observed in the parent compound **DICRO-1-Ni-i**.<sup>12c</sup> Each Cr atom adopts tetrahedral geometry with O–Cr–O bond angles ranging from 106.3(13)–114.78(11)°; while the Cr–O–Cr angle is 141.6(2)°. The Ni–O–Cr angles are acute at 166.8(8)°, as seen in chromate pillared **mmo** nets. The four organic linker ligands, which generate the equatorial plane, bridge to adjacent  $\text{Ni}^{2+}$  cations, resulting in a 2D (4,4) square lattice (**sql**). Two oxygen atoms from each  $\text{Cr}_2\text{O}_7^{2-}$  anion are coordinated to two  $\text{Ni}^{2+}$  cations from different **sql** layers, thereby pillaring the **sql** layers and generating the observed **pcu** network.

While self-assembly of judiciously chosen “nodes” and “linkers” can afford MOMs with predictable network topologies, control over the presence, mode and level of interpenetration remains a challenge.<sup>13</sup> This is exemplified by interpenetrated 2D square lattices (**sql**) and pillared square grids, which exhibit primitive cubic topology (**pcu**) and are also susceptible to interpenetration. Interpenetrated nets are of topical interest because interpenetration can profoundly affect bulk properties such as luminescence<sup>7</sup> and gas sorption.<sup>14</sup> When referring to topology nomenclature for interpenetration, it has been suggested that the RCSR 3-letter code should be modified with a **-c** extension to signify catenation.<sup>15</sup> However, this designation does not address the mode of interpenetration. The novel mode of interpenetration is therefore analysed using Hopf ring network (HRN) analysis, which can differentiate between modes of interpenetration. Interpenetrated

**pcu** then becomes **pcu-c**. While beyond the scope of this article, investigations into controlling interpenetration have been explored elsewhere.<sup>16</sup>

Interpenetration is particularly relevant with respect to gas sorption because it can lead to the formation of ultramicropores which enhance sorption performance, and, when controlled, allows for comparison between interpenetrated and non-interpenetrated variants of the same compound (polymorphs). Enhanced sorption performance is particularly seen when the pore structure is such that pores are lined by highly electrostatic inorganic species. In such a situation, the small pore diameter means that the adsorbate is necessarily confined to a cavity that is only slightly larger than the kinetic diameter of the gas molecule itself. The adsorbate is thereby forced to interact with all walls of the cavity simultaneously as opposed to just a surface. When combined with the strong electrostatics of inorganic anions, new benchmarks for important parameters such as  $Q_{\text{st}}$  and selectivity can be achieved.<sup>8</sup>

A review of the literature reveals that all previous examples of 2-fold **pcu-c** networks exhibit interpenetration in which the linkers are parallel to one another, *i.e.* independent networks are shifted in a parallel direction to one another through translation. Individual networks in **DICRO-2-Ni-i** interpenetrate in such a way that the organic dipyriddy linker intersect one another at an angle of *ca.* 35° (see Fig. 2), suggesting translation and a rotation of the second framework in reference to the first. HRN analysis<sup>17</sup> was used to classify the interpenetration of **DICRO-2-Ni-i** by topological type. In HRN analysis, each strong ring in an individual network is replaced with a single node located at that ring's barycentre. This node is then connected to every node that is constructed from rings originating from the second network that catenate the first ring (see Fig. 2). In this way, the number of rings from one network that catenate each ring in the second network, leads to the connectivity of the node derived from the catenated ring. Therefore, the HRN topology reveals information on both the number and modes of catenation between two interpenetrating frameworks.

A survey of all known 2-fold interpenetrated **pcu-c** networks (*ca.* 300) revealed that only two modes of interpenetration had previously been reported. In the vast majority of cases (98%), the mode of interpenetration is such that each ring of one network is entangled with four similar rings from the second network (Fig. 2). This generates a HRN that is 4-c and adopts **nbo** topology. There have also been a handful of instances, involving bent ligands, which lead to 2-fold interpenetrated **pcu-c** systems in which the HRN adopts a 6-c net with **hxx** topology. **DICRO-2-Ni-i** represents the first example of a third pattern of interpenetration wherein rings from the two independent networks entangle to form a HRN that adopts a binodal 4,6-c network with previously unknown topology (Fig. 2). This new topology has point symbol  $(4^2 \cdot 6^3 \cdot 8)_2(4^4 \cdot 6^9 \cdot 8^2)$ .

In addition to the unique interpenetration mode, the key difference between **DICRO-1-M-i** and **DICRO-2-Ni-i** is that the latter incorporates a longer organic linker ( $\text{N} \cdots \text{N} \text{ 1} = \sim 7 \text{ Å}$ ;  $\text{2} = \sim 9 \text{ Å}$ ) because ligand **2** incorporates an alkynyl group that extends length and conjugation. The novel mode of interpenetration



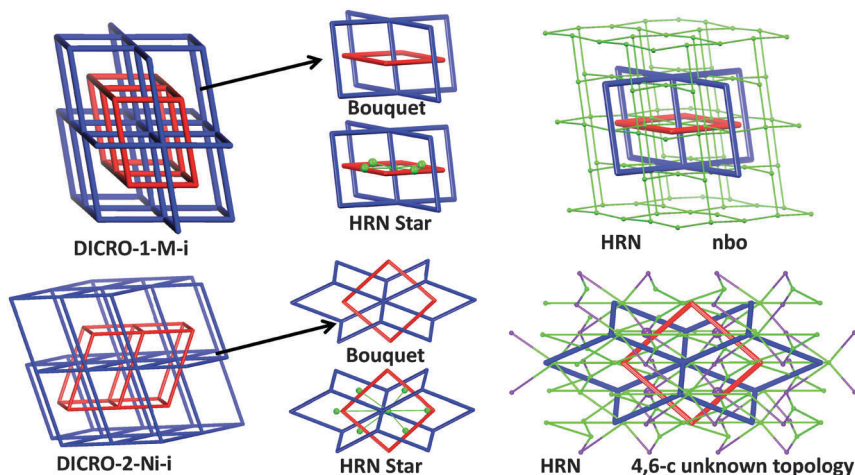


Fig. 2 Comparison of interpenetration in **DICRO-1-M-i** (top row) and **DICRO-2-Ni-i** (bottom row): left – scheme of interpenetration, centre – bouquet and HRN star, right – HRN topology.

between the two nets results in a 1D channel parallel with the *a*-axis with a pore diameter of *ca.* 3.6 Å. The permanent microporosity of **DICRO-2-Ni-i** was verified by N<sub>2</sub> sorption experiments performed at 77 K, where the apparent BET surface area was calculated to be 234 m<sup>2</sup> g<sup>−1</sup>. Based on liquid filling of N<sub>2</sub> at the saturated state, the uptake of 63.4 cm<sup>3</sup> g<sup>−1</sup> at *P/P*<sub>0</sub> = 0.25 corresponds to a pore volume of 0.091 cm<sup>3</sup> g<sup>−1</sup>, which is close to 0.094 cm<sup>3</sup> g<sup>−1</sup> calculated from single-crystal data. CO<sub>2</sub> sorption isotherms of **DICRO-2-Ni-i** at 273, 283 and 293 K were conducted and are presented in Fig. 3. CO<sub>2</sub> uptakes of 26.0, 23.4 and 19.9 cm<sup>3</sup> g<sup>−1</sup> were measured at 1 bar and 273, 283 and 293 K, respectively. The N<sub>2</sub> uptake at 1 bar and 293 K was observed to be only 2.6 cm<sup>3</sup> g<sup>−1</sup>. For a gas mixture at 1 bar comprised of 85% N<sub>2</sub> and 15% CO<sub>2</sub>, the selectivity predicted using Ideal Adsorbed Solution Theory<sup>18</sup> for **DICRO-2-Ni-i**, based on the single-component CO<sub>2</sub> and N<sub>2</sub> sorption isotherms at 293 K, was calculated to be 41. **DICRO-2-Ni-i** should therefore exhibit selective adsorption for CO<sub>2</sub> over N<sub>2</sub> (Fig. S8, ESI†) and with higher selectivity than compounds such as **HKUST-1** (20.1)<sup>19</sup> and **SIFSIX-2-Cu** (13.7).<sup>8c</sup>

In order to evaluate the strength of interaction between CO<sub>2</sub> and the framework, the CO<sub>2</sub> isotherms measured at 273,

283 and 293 K were fitted using the virial equation (Fig. S6, ESI†), and the isosteric heats of adsorption (*Q*<sub>st</sub>) were calculated using the Clausius–Clapeyron equation. The enthalpy at zero loading for **DICRO-2-Ni-i** is 30.5 kJ mol<sup>−1</sup> (Fig. S7, ESI†). This value is consistent with values observed in other classes of MOMs with **pcu** topology type incorporating hexafluorometallate as linear inorganic anions for pillars, **SIFSIX-2-Cu-i** (31.9 kJ mol<sup>−1</sup>),<sup>8c</sup> **TIFSIX-1-Cu** (26.5 kJ mol<sup>−1</sup>)<sup>8d</sup> and **SNIFSIX-1-Cu** (26.5 kJ mol<sup>−1</sup>).<sup>8d</sup> However, the *Q*<sub>st</sub> of **DICRO-2-Ni-i** is much smaller than that of **CROFOUR-1-Ni** (*ca.* 50 kJ mol<sup>−1</sup>),<sup>8b</sup> a HUM with **mmo** topology, and **SIFSIX-3-Zn** (45 kJ mol<sup>−1</sup>).<sup>8e</sup> The *Q*<sub>st</sub> in **CROFOUR-1-Ni** was validated using molecular simulations, which indicate that electrostatics of the exposed oxygen atoms of the CrO<sub>4</sub><sup>2−</sup> anion results in attraction towards CO<sub>2</sub> that is enhanced by induced polarisation. That **DICRO-2-Ni-i** exhibits weaker attraction for CO<sub>2</sub> than the aforementioned HUMs could be attributed to structural orientation, electrostatic effects or both. In **DICRO-2-Ni-i**, the dichromate anions are orientated in such a way that they do not protrude into the channel thought to be the site of CO<sub>2</sub> binding according to molecular simulations. This is in contrast with **CROFOUR-1-Ni**, in which the binding sites for CO<sub>2</sub> are lined by oxygen atoms of chromate anions. A similar situation exists in other high performing HUMs such as **SIFSIX-3-Zn**<sup>8c</sup> and **SIFSIX-3-Cu**,<sup>8e</sup> whereby the cavities accessible to the CO<sub>2</sub> are lined with highly electrostatic inorganic anions.

Molecular simulations of CO<sub>2</sub> adsorption in **DICRO-2-Ni-i** have been performed and indicate that CO<sub>2</sub> molecules adsorb into the accessible 1D channel as viewed along the *a*-axis of the crystal structure (Fig. 4). The simulations reveal that the small pore size (3.6 Å diameter), a consequence of interpenetration, generates tight packing of CO<sub>2</sub> molecules within the channel. The simulations also reveal the absence of interactions between oxygen atoms of Cr<sub>2</sub>O<sub>7</sub><sup>2−</sup> anions and guest CO<sub>2</sub> molecules, likely due to inaccessibility, which could explain the lower than expected *Q*<sub>st</sub> value of 30 kJ mol<sup>−1</sup> (~20 kJ mol<sup>−1</sup> lower than **CROFOUR-1-Ni**).

In summary, a new 3D hybrid ultramicroporous material (HUM), **DICRO-2-Ni-i**, has been constructed using dichromate

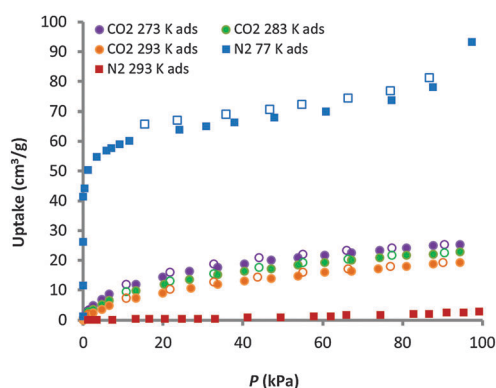


Fig. 3 Single component gas adsorption (filled symbols) and desorption (empty symbols) isotherms for **DICRO-2-Ni-i**.

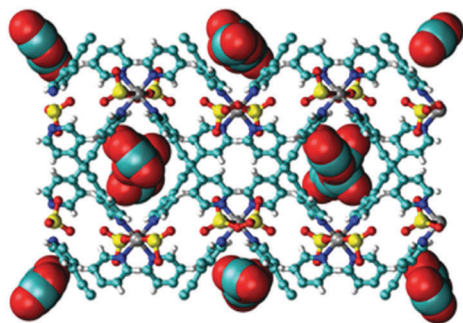


Fig. 4 The *a*-axis view of the modelled  $3 \times 2 \times 1$  system cell of **DICRO-2-Ni-i** at  $\text{CO}_2$  saturation. Atom colours: C = cyan, H = white, N = blue, O = red, Cr = yellow, Ni = silver.

anions as pillars to cross-link square lattices (**sql**) into a **pcu-c** network. This compound is the first example of 2-fold inclined interpenetration in **pcu-c** frameworks. This unique mode of interpenetration, complete with a new Hopf ring network topology, affords a distinct ultramicroporous 1D channel within the structure. Structural analysis, gas sorption experiments and molecular simulations indicate this channel is just large enough to adsorb molecules of  $\text{CO}_2$ . Additionally, molecular simulations suggest that  $\text{CO}_2$  molecules are confined to the ultramicroporous channels and are effectively isolated from interacting with the strongly electrostatic dichromate anions. Isolation of the  $\text{CO}_2$  molecules from the dichromate anions likely results in the somewhat lower than expected  $Q_{\text{st}}$  when compared with similar HUMs, which we attribute to very different pore chemistry. Future work will focus upon expanding the **DICRO-X-M** platform and further examples of **pcu-c** HUMs constructed using  $\text{Cr}_2\text{O}_7^{2-}$  in order to evaluate the effect of this anionic inorganic pillar upon gas sorption performance. The incorporation of a second metal centre (chromium) into these porous systems also offers the prospect of introducing a secondary function, including heterogeneous catalysis or redox behaviour.

M.J.Z. acknowledges SFI (13/RP/B2549), and B.S. acknowledges the National Science Foundation (Award No. CHE-1152362). Computational resources were made available by XSEDE Grant No. TG-DMR090028. The use of the services provided by Research Computing at the University of South Florida is also acknowledged.

## Notes and references

- (a) G. R. Desiraju, *The Design of Organic Solids*, Elsevier, Amsterdam, 1989; (b) B. Moulton and M. J. Zaworotko, *Chem. Rev.*, 2001, **101**, 1629.
- J. J. Perry, IV, J. A. Perman and M. J. Zaworotko, *Chem. Soc. Rev.*, 2009, **38**, 1400.
- (a) S. R. Batten, S. M. Neville and D. R. Turner, *Coordination Polymers Design, Analysis and Application Introduction*, RSC Publishing, Cambridge, UK, 2009; (b) *Metal–Organic Frameworks: Design and Application*, ed. L. R. MacGillivray, John Wiley & Sons, Hoboken, USA, 2010.
- (a) J. R. Li, R. J. Kuppler and H. C. Zhou, *Chem. Soc. Rev.*, 2009, **38**, 1477; (b) J. Liu, P. K. Thallapally, B. P. McGrail and D. R. Brown, *Chem. Soc. Rev.*, 2012, **41**, 2308; (c) L. J. Murray, M. Dinca and J. R. Long, *Chem. Soc. Rev.*, 2009, **38**, 1294; (d) K. Sumida, D. L. Rogow, J. A. Mason, T. M. McDonald, E. D. Bloch, Z. R. Herm, T. H. Bae and J. R. Long, *Chem. Rev.*, 2012, **112**, 724; (e) P. K. Thallapally, J. W. Grate and R. K. Motkuri, *Chem. Commun.*, 2012, **48**, 347; (f) Z. Zhang, Z.-Z. Yao, S. Xiang and B. Chen, *Energy Environ. Sci.*, 2014, **7**, 2868.
- (a) J. Lee, O. K. Farha, J. Roberts, K. A. Scheidt, S. T. Nguyen and J. T. Hupp, *Chem. Soc. Rev.*, 2009, **38**, 1450; (b) L. Q. Ma, C. Abney and W. B. Lin, *Chem. Soc. Rev.*, 2009, **38**, 1248.
- B. L. Chen, S. C. Xiang and G. D. Qian, *Acc. Chem. Res.*, 2010, **43**, 1115.
- M. D. Allendorf, C. A. Bauer, R. K. Bhakta and R. J. T. Houk, *Chem. Soc. Rev.*, 2009, **38**, 1330.
- (a) M. H. Mohamed, S. K. Elsaïdi, T. Pham, K. A. Forrest, B. Tudor, L. Wojtas, B. Space and M. J. Zaworotko, *Chem. Commun.*, 2013, **49**, 9809; (b) M. H. Mohamed, S. K. Elsaïdi, L. Wojtas, T. Pham, K. A. Forrest, B. Tudor, B. Space and M. J. Zaworotko, *J. Am. Chem. Soc.*, 2012, **134**, 19556; (c) P. Nugent, Y. Belmabkhout, S. D. Burd, A. J. Cairns, R. Luebke, K. Forrest, T. Pham, S. Q. Ma, B. Space, L. Wojtas, M. Eddaoudi and M. J. Zaworotko, *Nature*, 2013, **495**, 80; (d) P. Nugent, V. Rhodus, T. Pham, B. Tudor, K. Forrest, L. Wojtas, B. Space and M. J. Zaworotko, *Chem. Commun.*, 2013, **49**, 1606; (e) O. Shekhah, Y. Belmabkhout, Z. J. Chen, V. Guillermin, A. Cairns, K. Adil and M. Eddaoudi, *Nat. Commun.*, 2014, **5**.
- (a) M. Fujita, Y. J. Kwon, S. Washizu and K. Ogura, *J. Am. Chem. Soc.*, 1994, **116**, 1151; (b) R. W. Gable, B. F. Hoskins and R. Robson, *J. Chem. Soc., Chem. Commun.*, 1990, 1677.
- (a) S. Subramanian and M. J. Zaworotko, *Angew. Chem., Int. Ed.*, 1995, **34**, 2127; (b) S.-I. Noro, R. Kitaura, M. Kondo, S. Kitagawa, T. Ishii, H. Matsuzaka and M. Yamashita, *J. Am. Chem. Soc.*, 2002, **124**, 2468.
- F. H. Allen, *Acta Crystallogr., Sect. B: Struct. Sci.*, 2002, **58**, 380.
- (a) X. Y. Chen, B. Zhao, P. Cheng, B. Ding, D. Z. Liao, S. P. Yan and Z. H. Zhang, *Eur. J. Inorg. Chem.*, 2004, 562; (b) Y. Hayashi, T. Tagami, H. Mano and A. Uehara, *Chem. Lett.*, 2001, 562; (c) A. L. Kopf, P. A. Maggard, C. L. Stern and K. R. Poeppelmeier, *Acta Crystallogr., Sect. C: Cryst. Struct. Commun.*, 2005, **61**, M165.
- (a) S. R. Batten and R. Robson, *Angew. Chem., Int. Ed.*, 1998, **37**, 1460; (b) L. Carlucci, G. Ciani and D. M. Proserpio, *Coord. Chem. Rev.*, 2003, **246**, 247.
- (a) S. S. Han, D. H. Jung and J. Heo, *J. Phys. Chem. C*, 2013, **117**, 71; (b) J. Kim, S. T. Yang, S. B. Choi, J. Sim and W. S. Ahn, *J. Mater. Chem.*, 2011, **21**, 3070; (c) T. K. Prasad and M. P. Suh, *Chem. – Eur. J.*, 2012, **18**, 8673.
- M. O’Keefe, M. A. Peskov, S. J. Ramsden and O. M. Yaghi, *Acc. Chem. Res.*, 2008, **41**, 1782.
- (a) S. K. Elsaïdi, M. H. Mohamed, L. Wojtas, A. Chanthapally, T. Pham, B. Space, J. J. Vittal and M. J. Zaworotko, *J. Am. Chem. Soc.*, 2014, **136**, 5072; (b) L. Q. Ma and W. B. Lin, *J. Am. Chem. Soc.*, 2008, **130**, 13834; (c) O. Shekhah, H. Wang, M. Paradinas, C. Ocal, B. Schupbach, A. Terfort, D. Zacher, R. A. Fischer and C. Woll, *Nat. Mater.*, 2009, **8**, 481; (d) J. J. Zhang, L. Wojtas, R. W. Larsen, M. Eddaoudi and M. J. Zaworotko, *J. Am. Chem. Soc.*, 2009, **131**, 17040; (e) H. Aggarwal, P. M. Bhatt, C. X. Bezuïdenhout and L. J. Barbour, *J. Am. Chem. Soc.*, 2014, **136**, 3776; (f) C. T. He, P.-Q. Liao, D.-D. Zhou, B.-Y. Wang, W.-X. Zhang, J.-P. Zhang and X.-M. Chen, *Chem. Sci.*, 2014, **5**, 4755.
- E. V. Alexandrov, V. A. Blatov and D. M. Proserpio, *Acta Crystallogr., Sect. A: Found. Crystallogr.*, 2012, **68**, 484.
- A. L. Myers and J. M. Prausnitz, *AIChE J.*, 1965, **11**, 121.
- Q. Y. Yang, C. Y. Xue, C. L. Zhong and J. F. Chen, *AIChE J.*, 2007, **53**, 2832.